Nuclear Instruments and Methods in Physics Research A296 (1990) 744–748
North-Holland

PAPA, A PARTICLE TRACING CODE IN PASCAL

Eltjo H. HASELHOFF and Gerard J. ERNST

The Netherlands' Center for Laser Research, University of Twente, P.O. Box 217, 7500 AE Enschede, The Netherlands

During the design of a 10 μm high-gain FEL oscillator (TEUFEL Project) we developed a new particle-tracing code to perform simulations of thermionic- and photo-cathode electron injectors/accelerators. The program allows predictions of current, energy and beam emittance in a user-specified linac configuration. This paper describes the setup and the mathematical model of the program and shows some results as an illustration.

1. Introduction

The need for a new particle-tracing code arose because existing programs appeared to be modified so often that they had lost their continuity and clarity. Generally, documentation was poor and the mathematical model and used approximations were unknown. Furthermore, many scientific computer codes find their origin in the early seventies, and tend to have a rather old-fashioned setup compared to modern computer standards. This fact made the creation of a completely new program preferable to modification of the existing codes.

PAPA stands for a particle-tracing code in Pascal. The current version offers a solid base for a new, modern and convenient particle-tracing code, to be used for simulations of all kinds of linear-accelerator applications.

Keywords for PAPA are:
- modern, clear and consistent programming style,
- extensive explications in source code,
- modular setup – flexibility,
- ease in use,
- good documentation,
- Pascal compatibility.

To keep the Pascal syntax compatible to different compilers, we only used "standard" Pascal statements and avoided the use of excessive statements, as used in e.g. Borland's TurboPascal. Especially when used on a personal computer this approach unfortunately cancels much of the power and charm of modern compilers. For this reason the actions taken by PAPA are restricted to the creation of an ASCII output file, containing the input parameters and program output at discrete time intervals.

To process the data, we load the output file into an IBM-compatible PC, where it is converted by a number of TurboPascal programs to create all kinds of graphics in a fast and convenient way. One option that is worth mentioning is the creation of a perspective red–green view on an EGA/VGA monitor, which allows the user to see a true 3D presentation of the electron trajectories, using red–green glasses. Since these routines are more hardware-dependent and require only standard programming techniques, we do not discuss them here any further.

2. Brief discussion of the program flow

The program comes as a handful of include files, each of which contains one or several modules controlled by one main program which is very short. Each module contains an explanatory text describing what "goes in" and what "comes out". Fig. 1 is a simplified overview of the program's main procedures. The user can specify an arbitrary electron pulse and a configuration of rf cells, magnetic fields and electrostatic fields, by means of a simple code in an ASCII file. The field distribution inside rf cavities is read in from external ASCII files as well. We did not use Fourier coefficients, because it is not as fast and less accurate, although it can save quite an amount of RAM. Maybe is will be implemented in future versions. The entire mathematical model is contained in block number 12 and blocks number 14–16, describing how the electromagnetic interactions take place. The number of devices that can be specified is limited yet, but can be extended by just adding modules to the row 14/15/16. The numerical routines (11 or 19) do nothing else than solving a set of N variables, of which the first-order time derivatives are known (block 12). They can easily be replaced by any other routine.

3. Particle dynamics

In the PAPA code, an electron pulse is represented by a limited number of uniformly charged, rigid clouds,

Elsevier Science Publishers B.V. (North-Holland)

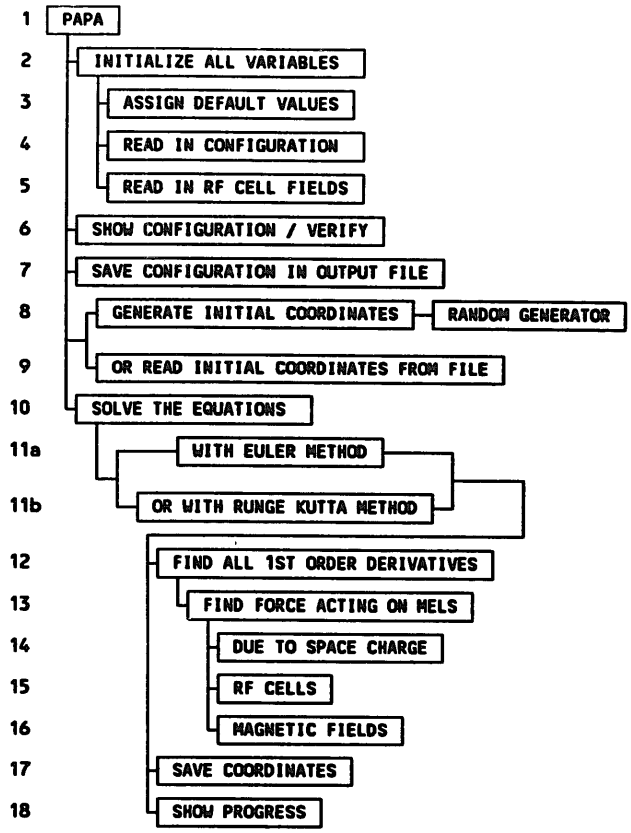

Fig. 1. Simplified overview of the program's hierarchy.

called mels (which stands for "macro-electrons"). The mels have a spherical shape in the lab frame. Although rigid, the spheres are not solid, which means that they are allowed to merge into each other. Their radius is calculated by PAPA for every time step as to make the total volume of all spheres equal to the total volume of the electron pulse. This radius is then multiplied by a user-specified factor, DMR (Decreases Mel's Radius). When the DMR is chosen to be zero, the mels will behave like point charges. PAPA uses mels rather then point charges, to prevent exaggerated force interactions when two mels come very close to each other. The mel approximation compensates for this, since, when the distance between two mels becomes zero (that is: they overlap completely), the repelling force between them is also zero. At the same time the recalculation of the mels' radius for every time step eliminates limitations of force interactions. Simulations have shown that this approach reduces significantly the dependence of the results on the number of particles.

To determine the radius of the mels, PAPA starts with finding a cylinder of length L and radius R_c in which the main part of the mels fit. The volume of this cylinder is given by

$$V = \pi R_c^2 L. \tag{1}$$

The length L is found by averaging over all N mels. If we assume that the mels are traveling in the (positive) z-direction, it is easily seen that a representative value for L can be found by

$$L = 4 \sum_{n=1}^{N} |\bar{z} - z_n|, \tag{2}$$

where $$\bar{z} \equiv \frac{1}{N} \sum_{n=1}^{N} z_n. \tag{3}$$

A value for the cylinder's radius R_c could be determined in a similar way by averaging over R_n, where $R_n = (x_n^2 + y_n^2)^{1/2}$ and x_n and y_n are the x- and y-coordinates of successive mels, but there is another way which avoids the calculation of the square root and the multiplications in the above equation and is therefore faster.

If we want to express the average x-coordinate of a uniform distribution of points in the half circle defined by

$$\{(x, y) \mid x^2 + y^2 \le R_c^2,\ x \ge 0\},$$

we find

$$\bar{x} = \frac{2}{\pi R_c^2} \int_0^{R_c} \int_{-\pi/2}^{\pi/2} r \cos(\phi) r \, dr \, d\phi = \frac{4R_c}{3\pi},$$

which leads to $R_c = 3\pi/4\bar{x}$. PAPA finds R_c by calculating

$$R_c = \frac{3\pi}{4N} \sum_{n=1}^{N} |x_n|. \tag{4}$$

If we want to have the volume of all mels together equal to V, as given in eq. (1), we must have

$$N \tfrac{4}{3} \pi R^3 = \pi R_c^2 L \Rightarrow R = \left(\frac{3R_c^2 L}{4N} \right)^{1/3}, \tag{5}$$

with L and R_c as expressed in eqs. (2) and (4), respectively.

The force reduction for nearby mels is done as follows. The thin line in fig. 2 shows the force between

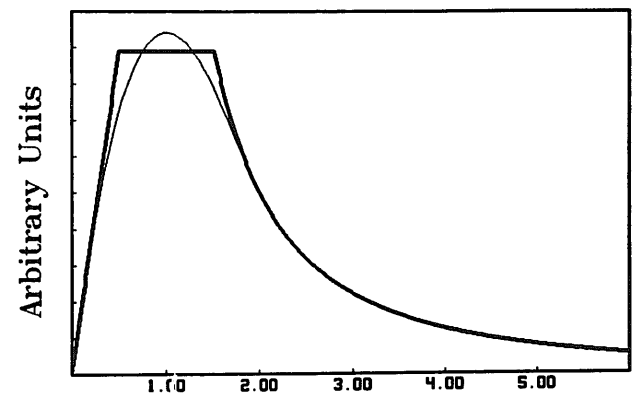

Fig. 2. Repelling force (arbitrary units) between two homogeneously charged rigid spheres with radius R as a function of r/R, r being the distance between the centers. Thin line: exact solution (computer calculus); thick line: PAPA approximation.

two uniformly charged, rigid but not solid, spherical clouds (radius R), as a function of the scaled distance r/R between their centers. The plot was obtained by a simple numerical method on a PC. When $r > 2R$, that is, the spheres do not "touch" each other, the force will be proportional to $1/r^2$, which follows directly from Gauss' theorem. When they overlap completely ($r = 0$), the repelling force is zero. The actual expression for the force is rather complicated, so PAPA uses the (fast) approximation as given by the thick line in fig. 1, which is defined by

$$\begin{aligned} &\frac{8}{9R^3}r && \text{for } 0 < \frac{r}{R} \le \tfrac{1}{2}, \\ &\frac{4}{9R^2} && \text{for } \tfrac{1}{2} < \frac{r}{R} \le \tfrac{3}{2}, \\ &\frac{1}{r^2} && \text{for } \tfrac{3}{2} < \frac{r}{R}. \end{aligned}$$

The motion of the mels is described by the Lorentz-force equations [mks units]:

$$\frac{\mathrm{d}}{\mathrm{d}t}(\gamma m \boldsymbol{v}) = -e(\boldsymbol{E} + \boldsymbol{v} \times \boldsymbol{B}) = \boldsymbol{F}, \tag{6}$$

$$\frac{\mathrm{d}}{\mathrm{d}t}(\gamma m c^2) = -e(\boldsymbol{v} \cdot \boldsymbol{E}) = \boldsymbol{v} \cdot \boldsymbol{F}, \tag{7}$$

where γ is the relativistic factor, m the mass of the mel, v its velocity, $-e$ its charge, $\boldsymbol{E}$ the electrical field, $\boldsymbol{B}$ the magnetic field, $\boldsymbol{F}$ the total force acting on the mel and c the velocity of light. (Eq. (7) gives no extra information, but is added for ease.) The set of equations (6) and (7) will now be written in a more convenient form. If we define $\boldsymbol{p} \equiv \gamma m \boldsymbol{v}$, eq. (6) can be written as

$$\frac{\mathrm{d}}{\mathrm{d}t}(\boldsymbol{p}) = \boldsymbol{F}. \tag{8}$$

Instead of using eq. (7), one may directly write down an expression for γ in terms of $\boldsymbol{p}$:

$$\gamma = \left(\frac{|\boldsymbol{p}|^2}{m^2 c^2} + 1 \right)^{1/2}. \tag{9}$$

In order to describe the mels' motion completely, we have to add

$$\frac{\mathrm{d}}{\mathrm{d}t}(\boldsymbol{r}) = \frac{\boldsymbol{p}}{m\gamma}, \tag{10}$$

where $\boldsymbol{r} \equiv (x, y, z)$ represents the mel's position.

Determining $\boldsymbol{F}$ as a function of the configuration, the mels' positions and velocities and the time, PAPA solves eqs. (8), (9) and (10) for each of the N mels.

4. Space-charge forces

Forces due to rf cavities and magnetic fields are easily implemented in eqn. (8). Space-charge effects are more complex. They are the most computing-time-consuming forces, since they are calculated for each integration step, and require a handful of multiplications for all possible combinations of two mels (point-by-point space-charge calculations).

The expression for the electromagnetic field created by a mel moving with *uniform velocity* is given by [1]

$$\boldsymbol{E} = \frac{1}{4\pi\epsilon_0} \frac{Q\boldsymbol{r}}{\gamma^2 s^3}$$

and (11)

$$\boldsymbol{B} = \frac{1}{c^2} \boldsymbol{v} \times \boldsymbol{E},$$

with

$$s \equiv r\left(1 - \frac{v^2}{c^2} \sin^2\theta\right)^{1/2}, \tag{12}$$

where $\boldsymbol{r}$ is the vector pointing from the mel to the place of observation, $\boldsymbol{v}$ the mel's velocity, Q its charge and θ the angle between $\boldsymbol{r}$ and $\boldsymbol{v}$.

If the mel is accelerated, the electromagnetic field has the form

$$\boldsymbol{E} = \frac{1}{4\pi\epsilon_0} \left\{ \frac{Q\boldsymbol{r}_{\mathrm{eff}}}{\gamma'^2 s^3} + \frac{Q\boldsymbol{r}' \times \left(\boldsymbol{r}_{\mathrm{eff}} \times \frac{\mathrm{d}\boldsymbol{v}'}{\mathrm{d}t} \right)}{c^2 s^3} \right\}, \tag{13}$$

$$\boldsymbol{B} = \frac{\boldsymbol{r}' \times \boldsymbol{E}}{r'c}, \tag{14}$$

where the quote stands for evaluating the retarded value and

$$\boldsymbol{r}_{\mathrm{eff}} \equiv \boldsymbol{r}' - \frac{r'\boldsymbol{v}'}{c}.$$

PAPA uses eq. (12) rather than eq. (13), which is not correct, but a convenient approximation. We will now make an estimate of the error. Comparing eqs. (12) and (13) we see that the relative error for the approximated value of $\boldsymbol{E}$ is

$$\frac{\delta E}{E} \cong \frac{\gamma^2 r}{c^2} \frac{\mathrm{d}v}{\mathrm{d}t}.$$

In a linac, acceleration of the mels is mainly caused by rf fields E_{rf}, so that we may write

$$\frac{\mathrm{d}(\gamma\beta)}{\mathrm{d}t} = \gamma^3 \frac{\mathrm{d}\beta}{\mathrm{d}t} = \frac{QE_{\mathrm{rf}}}{mc},$$

(where $\beta \equiv v/c$) so that we find

$$\frac{\delta E}{E} = \frac{QE_{\mathrm{rf}} r}{\gamma m c^2} = \frac{r}{\rho}, \tag{15}$$

where $\rho \equiv \gamma m c^2 / QE_{\mathrm{rf}}$. If we consider the case of an electric field of 100 MV/m and $\gamma = 1$, we find that $\rho \cong 5 \times 10^{-3} = 5$ mm. A typical value for the average distance between two mels is 1 mm, which will lead to a 20% error for the lowest energy. As seen from eq. (14), the error is proportional to $1/\gamma$. A typical value for the energy after a drift of 1 cm in a photocathode cell is 1

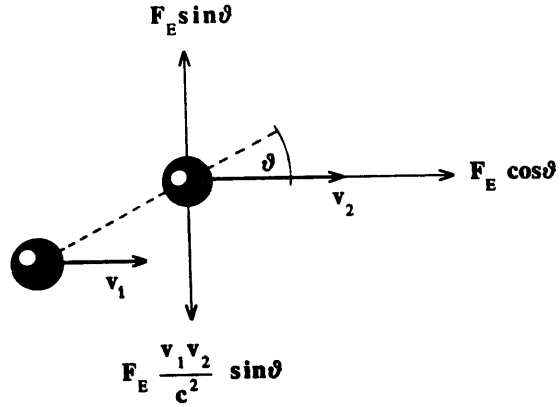

Fig. 3. Paraxial space-charge approximation (see text).

MeV, which corresponds to $\gamma = 3$. Thus the error will decrease rapidly when the particles are accelerated. Furthermore, the absolute error δE is proportional to $1/r\rho$, and will thus tend to be significant only when space-charge effects become negligible. The final accuracy will depend on the number of mels that are used and the parameters in eq. (14).

We emphasize the fact that in case of bending magnets, or perpendicular magnetic fields like in a microtron, the approximation will usually be insufficient. At the moment of this writing, we are developing a program which calculates the electrons' dynamics in a race-track microtron, and in this case the full expression (13) must be used when the electrons travel through the D's.

If perpendicular velocity components are negligible compared with the longitudinal velocity, $v_\perp \ll v_\parallel$, the expressions in eqs. (11) can be simplified as to speed up the computations considerably. Fig. 3 shows two mels, numbered 1 and 2, with (parallel) velocities v_1 and v_2. The electric force acting on mel 2 due to the presence of mel 1 is directed from mel 1 to mel 2 and can be written out in a perpendicular and a parallel component (with respect to the plane of the paper):

$$\boldsymbol{F}_E = \boldsymbol{F}_{E,\parallel} + \boldsymbol{F}_{E,\perp} = -e\left(\boldsymbol{E}_\parallel + \boldsymbol{E}_\perp\right). \tag{16}$$

It is easily shown that the paraxial approximation used with eq. (12) leads to the following force components:

$$\begin{aligned} \boldsymbol{F}_\perp &= \boldsymbol{F}_{E,\perp}\left(1 - \frac{v_1 v_2}{c^2}\sin\phi\right), \\ \boldsymbol{F}_\parallel &= \boldsymbol{F}_{E,\parallel}, \end{aligned} \tag{17}$$

where θ is the angle between v_2 and $\boldsymbol{F}_E$. Use of eqs. (17) rather than the full expressions as derived from eq. (12) avoids the computation of six multiplications for each cross product, and is considerably faster, especially for a large number of mels. The paraxial approximation will be sufficient in most cases. In the PAPA code both the complete and the paraxial space-charge routines are present.

5. The numerical routines

By means of a parameter in the input file, one may choose between two different numerical routines to solve eqs. (10) and (11): either first-order Euler or fourth-order Runge–Kutta extrapolation [2]. Most existing particle-tracing codes use the Euler method, which is not very accurate and often very unstable. The Runge–Kutta routine allows much larger time steps, which makes the calculations approximately 5–10 times faster.

6. Other options

By means of a parameter in the input file, it is possible to simulate mels emerging from a cathode surface, instead of just popping them in space at the beginning of the simulation. If an electrostatic field of an anode–cathode configuration is put in one of the cell field files, we expect that PAPA could also be used as a thermionic gun simulator, with the inclusion of pulse effects.

To reduce errors, the program (optionally) translates the code in the input files to plain English, before starting the calculation. It is also possible to have the specified rf fields mapped on the screen, as for easy verification.

Initial coordinates can be generated by the program (fig. 1, block 8), when some quantities like e.g. beam current and emittance are specified, or can be read from an ASCII text file (block 9). This allows combined use with other programs, and also eliminates the need to repeat an entire simulation from the beginning, if it gets stuck somewhere halfway.

The explanatory text in the program's code is closely related to the documentation. This makes modification of the code even easier.

7. Some results

Just to give an impression of what the program does, figs. 4a–c show the results of a 2 ns, 1 A electron pulse at 100 keV, with zero energy and angular spread, which is bunched by a 250 MHz, 40 kV rf cell. The cell is positioned at 21 cm, while the entire configuration was embedded in a 0.08 T magnetic guiding field. All the plots are screen dumps of our graphic routines on an Olivetti PC with ATT graphics.

Fig. 4a is a side view of the electron pulse (x- vs z-coordinate) at three different positions along the z-

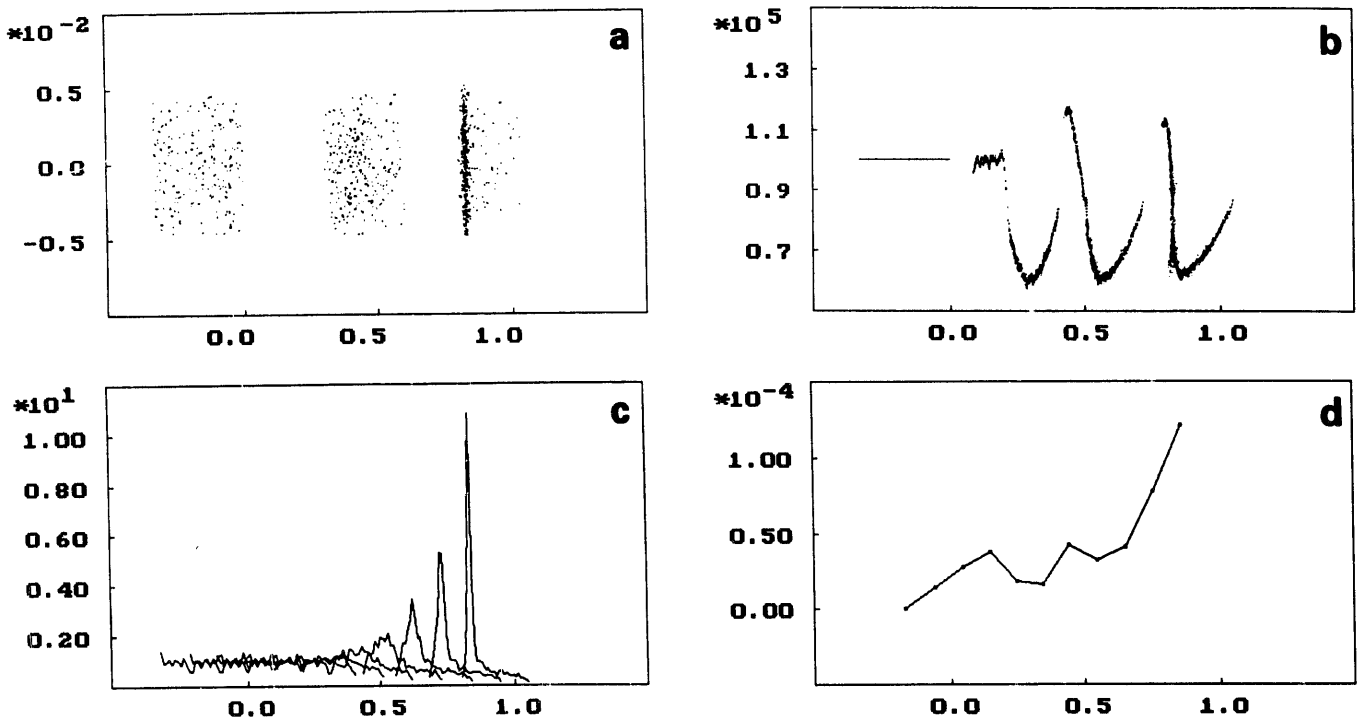

Fig. 4. (a) A typical simulation result (x-coordinate [m] vertical, z-coordinate [m] horizontal). A 2 ns, 100 keV, 1 A electron pulse with zero energy spread and zero emittance is compressed by a 40 keV, 250 MHz buncher. The picture shows the mels' distribution at three different positions along z. (b) The mels' energy [eV] as a function of z [m] for different positions along z [m]. (c) Current envelope [A] of the pulse for different positions along z [m]. (d) Rms emittance [mrad] as a function of the pulse's position along z [m].

axis. The initial bunch of about 35 cm (2 ns at 100 keV corresponding to $\beta = 0.55$) is compressed at a maximum at about 80 cm (rightmost pulse). Bunching seems to occur at the tail of the pulse, which can be explained by looking at fig. 4b, which shows the mels' energy as a function of their z-coordinate for four different positions along z. Obviously the initial phase of the rf cell was not perfect. The ripple at the tail of the second cluster from the left is caused by space-charge interactions. Fig. 4c shows the pulse's rms emittance in mrad along z, while fig. 4d gives the pulse current [A] along z. We see that the initial current of 1 A reaches a value of 10 A at about 80 cm.

8. Future actions

As we mentioned before, we are currently working on a similar program, of which input and output will be compatible with PAPA, which does a particle simulation of a racetrack microtron (RTM). We intend to use an RTM in combination with a photocathode gun, and the new code is meant to do predictions of the RTM's high-current behavior [3].

9. Conclusion

We have presented a new particle-tracing code, which is user-friendly, easily accessible and modern. The numerical procedures are flexible and faster than in most existing particle-tracing codes. It is to be considered a public-domain program, and its entire setup is devoted to the easy extension and modification by other users. Anyone who is interested can contact us at the above adress.

References

[1] J.R. Reitz, Foundations of Electromagnetic Theory (Addison–Wesley, 1979) chapter 21.

[2] W.C. Gear, Numerical Initial Value Problems in Ordinary Differential Equations (Prentice–Hall, Englewood Cliffs, NJ, 1971) chapter 2.

[3] G.J. Ernst et al., Proc. 10th Int. Free Electron Laser Conference, Jerusalem, Israel, 1988, Nucl. Instr. and Meth. A285 (1989) 71.